1216–1226 *Nucleic Acids Research, 2016, Vol. 44, No. 3* *Published online 13 January 2016*
doi: 10.1093/nar/gkv1484

The role of MatP, ZapA and ZapB in chromosomal organization and dynamics in *Escherichia coli*

Jaana Männik[1], Daniel E. Castillo[2], Da Yang[2], George Siopsis[2] and Jaan Männik[1,2,*]

[1]Department of Biochemistry and Cellular and Molecular Biology, The University of Tennessee, Knoxville, TN 37996-0840, USA and [2]Department of Physics and Astronomy, The University of Tennessee, Knoxville, TN 37996-1200, USA

Received August 21, 2015; Revised December 5, 2015; Accepted December 8, 2015

ABSTRACT

Despite extensive research over several decades, a comprehensive view of how the *Escherichia coli* chromosome is organized within the nucleoid, and how two daughter chromosomes segregate has yet to emerge. Here we investigate the role of the MatP, ZapA and ZapB proteins in organizing the replication terminus (Ter) region and in the chromosomal segregation process. Quantitative image analysis of the fluorescently labeled Ter region shows that the replication terminus attaches to the divisome in a single segment along the perimeter of the cell in a MatP, ZapA and ZapB-dependent manner. The attachment does not significantly affect the bulk chromosome segregation in slow growth conditions. With or without the attachment, two chromosomal masses separate from each other at a speed comparable to the cell growth. The separation starts even before the replication terminus region positions itself at the center of the nucleoid. Modeling of the segregation based on conformational entropy correctly predicts the positioning of the replication terminus region within the nucleoid. However, the model produces a distinctly different chromosomal density distribution than the experiment, indicating that the conformational entropy plays a limited role in segregating the chromosomes in the late stages of replication.

INTRODUCTION

The bacterial chromosome forms a compact structure, the nucleoid, where DNA is packed into a volume that is about 1000-fold smaller than the volume of the unconfined DNA coil (1). Although not surrounded by a nuclear membrane, the nucleoid only fills a part of the bacterial cytosol. A combination of factors involving supercoiling (2), osmotic pressure (3–5) and DNA binding proteins (6,7) have been implicated in the compaction of DNA within the cell. Although naked DNA, which is osmotically compacted and supercoiled, is expected to form a random branched polymer coil, the bacterial chromosome appears to take a much more orderly structure. In this ordered structure, specific chromosomal loci localize in a predictable way within the nucleoid in a cell-cycle dependent manner (1,8). In *Escherichia coli*, in slow growth conditions it is observed that the replication origin (Ori) positions itself at the center of the nucleoid in the beginning of the cell cycle (9). The chromosomal loci to the left and right of Ori localize to different cell halves. The physical distance of a locus from the nucleoid center has been shown to depend linearly on the genetic separation between this locus and the Ori (10). However, taking that the *E. coli* chromosome is not linear but circular, such positioning cannot apply to all genomic regions. It has been proposed that DNA around the replication terminus does not follow the same ordering, but stretches across the nucleoid and connects the left and right arms of the chromosome (9–12).

A linearly organized chromosome with a stretched out replication terminus region is at odds with other findings that suggest the *E. coli* chromosome is organized into distinct macro-domains (MDs). Here, an MD refers to a genomic region of about one mega-base size that is to some degree physically isolated from the rest of the chromosome and more compacted. Four MDs have been proposed; one surrounding the replication origin (Ori MD), another surrounding the replication terminus region (Ter MD) and two flanking the Ter MD from the left (Left MD) and the right (Right MD) (13–15). The Left and Right MDs are thought to be separated from the Ori MD by unstructured regions (14,15). While very little is known about the Ori, Left and Right MDs, recent studies have provided clues on how the Ter MD is organized. The main factor responsible for the organization of the Ter MD appears to be the DNA binding protein MatP (macrodomain Ter protein) (15). MatP binds specifically to a 13 bp sequence motif called *matS*. Notably, this sequence motif is found 23× (about every 35 kb) only in the replication terminus region, which is centered on the *dif* site, and nowhere else in the *E. coli* chromosome. According to *in vitro* studies, MatP can loop DNA between two *matS*

*To whom correspondence should be addressed. Tel: +1 865 974 6018; Fax: +1 865 974 7843; Email: JMannik@utk.edu

sites (16). In such loops, two MatP dimers, which are attached to two different *matS* sequences, bind to each other via their C-terminal domains. The resulting DNA loops can explain the compaction of the Ter MD and its spatial isolation from the rest of the chromosome.

In addition to its role in looping DNA, MatP also has been implicated in positioning the cell division apparatus with respect to the Ter MD through a positive regulation mechanism (17) and anchoring the Ter MD to the Z-ring through a linkage involving ZapA, ZapB and MatP (18). We refer to this linkage as the Ter linkage (19). Recent work has provided evidence that the Ter linkage consists of an extensive network of ZapB filaments which span about 100 nm from the Z-ring toward the nucleoid (20). One side of this network is linked to the Z-ring via ZapA, which is known to interact with FtsZ (21,22), and the other side to DNA in the replication terminus region via MatP (18,20).

Thus, the MatP protein has been implicated in two roles: (i) the cross-linking of DNA in the Ter MD (15) and (ii) linking the chromosome to the divisome together with ZapA and ZapB (18). Moreover, it is conceivable that MatP can also cross-link two daughter chromosomes after their replication. Here we explore how these links affect chromosome organization and segregation by eliminating different linkages, and observing chromosomal dynamics using live cell time-lapse microscopy. Our measurements show that the attachment of the Ter region to the divisome is dependent on all three proteins. However, MatP, compared to ZapA and ZapB, has a different effect on the compaction of DNA within the Ter region and its mid-cell positioning. While important in organizing the Ter region and holding it fixed at mid-cell, all three proteins have only a minor effect on the global chromosome segregation, which progresses largely independently of all aforementioned links. To further understand the segregation processes, we modeled the chromosomes as an entropic spring with excluded volume interactions following the approach by Jun *et al.* (23). Although the model can explain the mid-cell positioning of the Ter region, it fails to account for the bulk chromosomal density distribution, indicating that conformational entropy is not the main driver of chromosome segregation in the late stages of replication.

MATERIALS AND METHODS

Strains and growth conditions

All strains in this study were derivatives of *E. coli* MG1655 (Supplementary Table S1). In slow growth conditions, cells were cultivated in M9 minimal medium (MP Biomedicals) supplemented with magnesium sulfate and 0.3% glycerol. LB medium (Fischer Scientific) was used for fast growth. 20 μg/ml kanamycin and 34 μg/ml chloramphenicol were added to the growth medium for strains with respective resistance markers. All bacteria were grown and imaged at 28°C.

For still imaging, we used M9 and LB agarose pads, and for time lapse imaging, home-made glass bottom dishes. In time lapse imaging, cells were pipetted to #1.5 glass coverslips on the bottom of the dish and covered with a (about 0.5 cm thick) slab of M9 agarose with magnesium sulfate and 0.3% glycerol. No antibiotics were used in agarose during imaging.

Fluorescent microscopy and image analysis

A Nikon Ti-E inverted fluorescence microscope with a 100× NA 1.40 oil immersion phase contrast objective was used for imaging of the bacteria. Fluorescence was excited by a 200W Hg lamp through a ND4 neutral density filter. Chroma 41004 and 41001 filtercubes were used to record mCherry and YPET images, respectively. Images were captured by an Andor iXon DU897 camera, and recorded using NIS-Elements software.

Custom Matlab scripts based on the Matlab Image Analysis Toolbox, DipImage Toolbox (http://www.diplib.org/) and PSICIC program (24) were used for image analysis. In addition to Matlab, simpler image processing, such as contrast and brightness adjustments, were done using ImageJ software (v1.41o). Further details on image analysis can be found in the Supplementary Information Text.

Coarse grain molecular dynamics modeling

We simulated the *E. coli* chromosomes using a bead on a string model following the approach by Jun *et al.* (23,25). The beads interacted with each other and with the surrounding nucleoid boundary by a repulsive Lennard-Jones potential, and were held together by a FENE potential. A total of 150 beads of 80 nm diameter each represented a fully replicated chromosome. The 80 nm bead sizes were chosen following arguments put forward in (26,27). The beads were confined to a cylindrical volume, which was 7 bead diameters wide and 34 long representing approximately the size of an unreplicated nucleoid. For partially replicated chromosomes, the nucleoid length increased in proportion to the replicated nucleoid fraction. MatP cross-linking effects were accounted for by adding an attractive Lennard-Jones potential between all beads that constituted the Ter region. The strength of this potential was chosen so that the radius of gyration for the Ter region decreased by 30% after adding the potential. All calculations were performed using the ESPRESSO package (28).

RESULTS

When at mid-cell, the Ter region is stretched along the cell's short axis

In previous reports, localization patterns of the Ter region along the *long* axis of the cell have been described at various points in the cell cycle (15,17,18). These measurements have shown that the Ter region moves from the vicinity of the new pole to mid-cell early in the cell cycle and stays in this location for the majority of the cell cycle before splitting into two just before the cell division. Here, we first characterized the positioning of the replication terminus region along the *short* axis of the cell during the time when it is positioned at mid-cell. For that purpose, we constructed a strain where the whole chromosome was labeled by HupA-mCherry and the Ter region by MatP-YPET. Both constructs were expressed from their native promoters and appeared functional as they did not affect the growth rate of

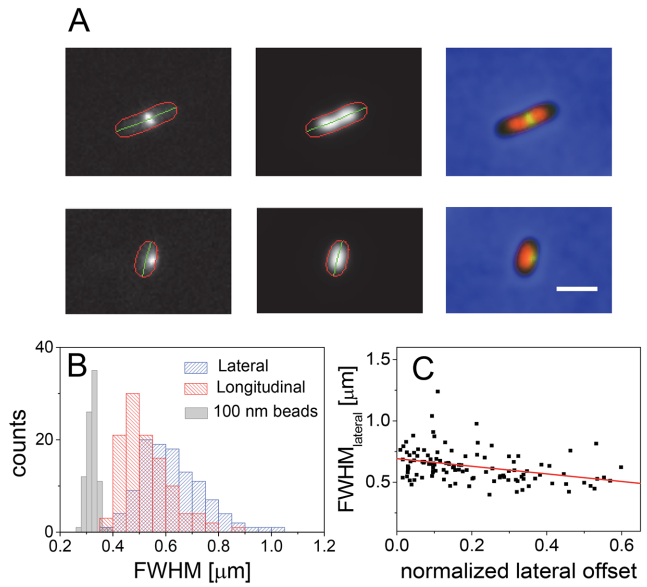

Figure 1. When at mid-cell, the Ter region is elongated along the short axis of the cell. (**A**) Images of two representative cells where the MatP-YPET labeled Ter region is localized at the center of the nucleoid. From left to right are fluorescent images of MatP-YPET, HupA-mCherry and a composite image where the two fluorescent images are overlaid with a phase contrast image. The latter is pseudo-colored blue for better contrast. The contours plotted in fluorescent images are cell boundaries (red) and midlines (green) as determined from phase contrast images. Scale bar is 2 μm. (**B**) Widths of MatP-YPET foci along long and short axes of cells. For comparison, shown also are widths measured from 100 nm fluorescent beads (solid gray fill). (**C**) Lateral width versus normalized offset of the focus from the cell center along short axes of cell. Cell radius is used for normalization. Solid line is a linear fit to the data (FWHM [μm] = 0.69–0.31x(normalized offset)).

the cells. The wild-type and labeled cells grow with an average doubling times of 117 ± 24 min and 104 ± 30 min, respectively. In many of these cells, the MatP-YPET labeled Ter region appeared elongated along the short axis of the cell (Figure 1A, top row), although in others circular foci were present (Figure 1A, bottom row). To characterize the elongation of the Ter region in these cells, we fitted two intensity line profiles of MatP-YPET fluorescence with Gaussians (Supplementary Information Text). One of these profiles followed the long axis of the cell (longitudinal profile) and the other the short axis (lateral profile). Consistent with the visual appearance, the widths in the lateral directions exceeded on average the widths in the longitudinal direction (Figure 1B). Note that the widths of the MatP-YPET profiles in both directions considerably exceeded the widths of profiles measured using 100 nm fluorescent beads (Life Technologies, Tetraspeck). The latter rules out that a significant contribution to the experimentally measured widths comes from the point spread function of the microscope. Lateral elongation of foci was also present when we used mCherry instead of YPET as a C-terminal fusion to MatP (Supplementary Figure S1).

The lateral widths of the MatP foci at mid-cell did not depend significantly on the cell length (Supplementary Figure S2). However, these widths were correlated with how much the centers of the MatP-YPET foci were offset from the cell's midline in the radial direction. When the center position of the focus was further away from the cell's midline, then the widths of the MatP foci were on average smaller (Figure 1C). This finding can be explained if one assumes that MatP-YPET is attached to the divisome along a single segment, which does not span the whole circumference of the cell. Depending on how this segment is oriented relative to the imaging plane the MatP-YPET focus in microscopic image appears either as a dot or as a short line (Supplementary Figure S3). The dot appears when the focus is at the periphery of the cell image and the short line when the segment is at the center of the cell. A relatively low correlation coefficient between the lateral width and offset of MatP foci (Figure 1C; $R = -0.36$) indicates that the length of the segment can vary significantly from cell to cell.

ZapA and ZapB play a differential role compared to MatP in organizing the Ter region at mid-cell

The Ter linkage that anchors the chromosome to the divisome includes MatP, ZapB and ZapA. These proteins have been reported to interact with each other in sequential order, MatP-ZapB-ZapA, i.e. ZapA interacts with ZapB, but not directly with MatP (18). Consequently, deletion of any of these proteins should eliminate the Ter linkage and the lateral elongation of the Ter foci. To test this hypothesis we introduced *zapA* and *zapB* deletions, and 20 amino acid truncation to the MatP C-terminal coiled-coil domain (*matPΔC*) in the WT strain that already carried HupA-mCherry and MatP-YPET labels. For respective cell images see Supplementary Figure S4. The 20 aa deletion of the C-terminal domain of MatP has been shown to abolish the interaction between MatP and ZapB, and also the MatP-MatP self-interaction, which is necessary for the formation of DNA loops (16,18). Consistent with the above hypothesis, the MatP foci in the *ΔzapB*, *matPΔC* and *ΔzapA* strains were not elongated in the lateral direction as in wild-type cells, but in the longitudinal direction (Supplementary Figure S5). The average lateral widths in all three deletion strains were essentially the same (Figure 2A), and significantly smaller than this width in wild-type strain ($P < 0.05$; *t*-test), consistent with the idea that all these proteins are required to form the Ter linkage. The difference in the lateral focal widths of the MatP-YPET and MatPΔC-YPET strains furthermore confirmed that the C-terminal fusion of YPET to MatP did not significantly affect the function of the protein. If the YPET fusion had affected the function of the C-terminal domain of MatP, then one would have expected these two strains to have similarly shaped MatP-YPET foci. Unlike the lateral width, the average longitudinal widths were longer for the deletion strains than for wild-type cells (Figure 2B). Interestingly, the average longitudinal widths in the *ΔzapA*, *ΔzapB* strains were both smaller than the width in the *matPΔC* strain ($P < 0.05$; *t*-test). The latter finding indicates that MatP has a different role compared to ZapA and ZapB in the compaction of the Ter region at mid-cell.

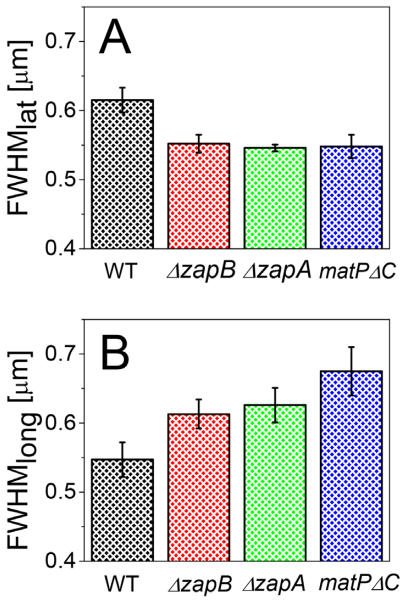

Figure 2. Widths of the Ter foci in longitudinal and lateral directions. (**A**) Average lateral widths for WT, *ΔzapB*, *ΔzapA* and *matPΔC* strains. For each strain, three replicate measurements were averaged. The error bars are s.e.m. based on the replicate measurements. Each replicate measurement includes data from about 100 cells. (**B**) The same measurements in longitudinal direction.

Constriction at the center of the nucleoid precedes centralization of MatP focus

Next, we investigated how the localization and organization of the Ter region correlates with the morphological changes of the whole chromosome throughout the cell cycle. For illustrative purposes, we first describe processes based on one typical cell before discussing population average data. As observed earlier (15,17,18), the Ter region is localized near the new pole at the periphery of the nucleoid at the beginning of the cell cycle (Figure 3A and B). This pattern appears inconsistent with the notion that the Ter region is spread throughout the nucleoid at the early stages of the cell cycle and connects the left and right replichores. However, during this period, the MatP-YPET focus typically has an asymmetric shape with an extended tail that reaches to the center of the nucleoid (Figure 3C, $t = 0$, 8 min). The presence of the tail may indicate that while part of the Ter region forms a compact unit, part of it is stretched and spans over about half of the nucleoid.

After the initial localization at the nucleoid periphery, the majority of the Ter region moves to the nucleoid center (Figure 3C, $t = 16$ min). This movement coincides approximately with the transition from a compact to a bi-lobed nucleoid morphology. Here, compact signifies essentially uniform featureless distribution of the nucleoid mass, while the characteristic of a bi-lobed shape is a constricted region at the center of the nucleoid. In the intensity line profiles of HupA-mCherry, the constriction appears as a local minimum. We first hypothesized that the onset of the constriction may result from the cross-linking of the nucleoid center by MatP proteins. However, we abandoned this hypothesis because in many cells such as in Figure 3C ($t = 8$ min) the constriction in the nucleoid center appears before the Ter region moves from the nucleoid periphery to its center. Further quantification of this effect can be found in the next section (Figure 5A).

After the MatP-YPET labeled Ter region centralizes, it stays at the center of the nucleoid mass for most of the remaining cell cycle before splitting during the cell division (Figure 3D). Such positioning of the Ter region is in contrast to the rest of the chromosome, which separates into two distinct nucleoid masses that move apart from each other (Figure 3B; C, $t = 32$ min). These chromosomal masses become two new daughter nucleoids once replication of the Ter region is completed. As the cell grows, we observe both the nucleoid length and the cell length to increase exponentially in time (Figure 3D). It is possible that with better time resolution we would have resolved step-like increases in nucleoid length, as has been reported before (29), but here we have opted for lower time resolution to avoid bleaching of the MatP-YPET focus, and therefore report only the overall trend in nucleoid expansion. Exponential time-dependence in nucleoid movement is also evident from the decrease in nucleoid density at the center of the nucleoid (Figure 3E). Note that Figure 3E shows an average normalized decrease of density (modulation), as inferred from the HupA-mCherry line profiles for a population of cells ($N = 17$). The individual curves for the cells shown in Figure 3E can be found in Supplementary Figure S6. Thus, the measurements indicate an overall exponential expansion of the nucleoid length that is accompanied by an exponential reduction of the nucleoid density at the center of the nucleoid. The exponential decrease in nucleoid density starts on average before the Ter region centralizes.

The role of ZapA, ZapB and MatP in bulk chromosome segregation

Next we investigated how *zapA*, *zapB* and *matPΔC* deletions affected the formation of constrictions at the centers of nucleoids. We first followed one typical *matPΔC* cell (Figure 4A–D). Note that even though MatPΔC-YPET is not functional for cross-linking the chromosome and has lost its attachment to the divisome, it is possible to observe its focus throughout the cell cycle in most cells. Unlike in wild-type cells, the MatP-YPET focus appears much more dynamic in *matPΔC* cells. It can move as a single unit from one pole of the nucleoid to another (Figure 4C–D). Moreover, it can become diffuse and then condense again or it can occasionally split into two. However, for all cells where we carried out an analysis similar to the one shown in Figure 4A–D ($N = 18$), we found that there is some period in the cell cycle where a compact MatP focus is localized at the center of the nucleoid (cf. Figure 4C, $t = 56$ min). As in the wild-type strain, we observed that the centralization of the MatP focus was frequently preceded by the formation of constriction at the center of the nucleoid (Figure 4C, $t =$ 40 min). Similar to the wild-type strain, the constriction at the center of the nucleoid and associated minimum in intensity line profiles, also grows exponentially in time for a large fraction of the cell cycle (Figure 4E, Supplementary Figure S6B and D).

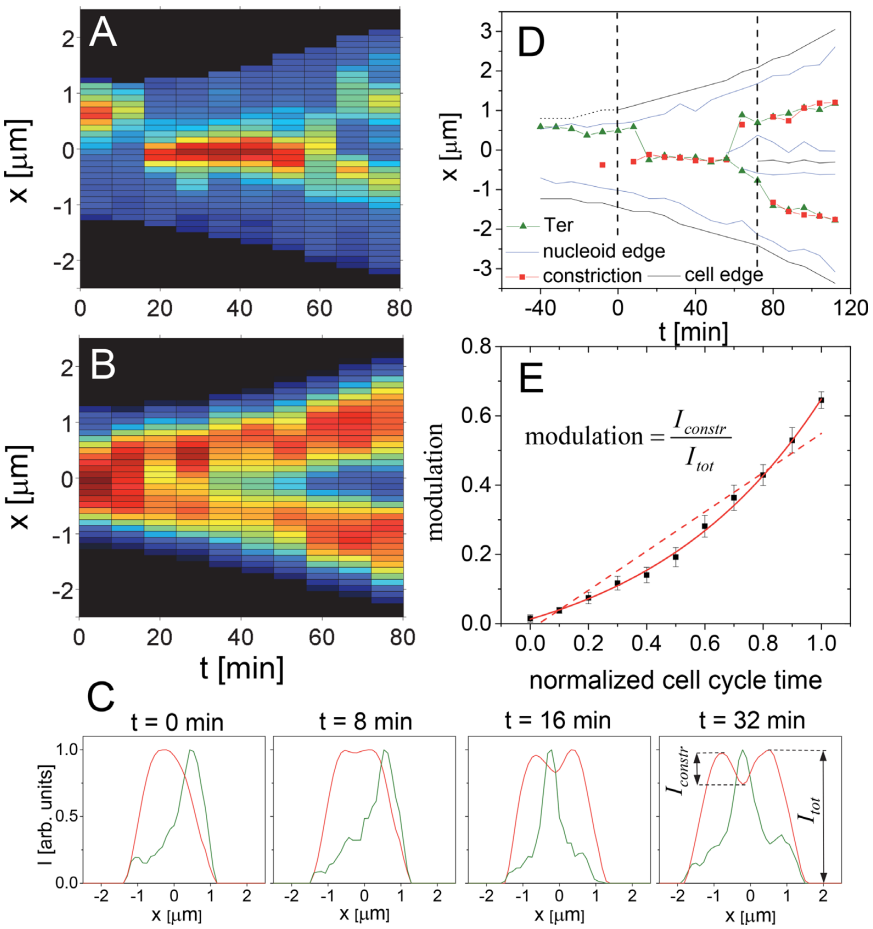

Figure 3. Dynamics of the MatP-YPET focus and the chromosome in wild-type cells. (**A**) Intensity distribution of MatP-YPET along the long axis for a representative cell during one cell cycle. Red corresponds to high and blue to low fluorescence intensity. Black regions are outside the cell. (**B**) HupA-mCherry intensity distribution for the same cell. (**C**) Intensity line profiles of both labels along the long axis of this cell at the beginning of the cell cycle. All profiles are normalized by their maximum values. (**D**) Contours of cell edges (black solid line), nucleoid edges (blue solid lines), centroids of MatP-YPET labeled Ter regions (filled triangles) and locations of minima in chromosomal densities (red squares) for the same cell. Dashed vertical lines indicate the timing of cell division. Note that the cell was tracked also before its birth and after its division. Before the birth, the center of the constriction in mother cell was taken as the cell edge (dotted black line). (**E**) Normalized depth of the minimum in intensity distribution of nucleoid label at the center of the nucleoid as a function of normalized cell cycle time. Data are an average from 17 time-lapse sequences from different cells. Error bars represent s.e.m. Solid line is exponential and dashed line linear fit.

Common to all three deletion strains and wild-type cells were two observations. First, for at least some period of the cell cycle, the MatP-YPET focus stays at the center of the nucleoid. Second, for a significant fraction of the cells, the constriction at the center of the nucleoid appears before the MatP-YPET focus moves to the center of the cell. The fraction was the largest for wild-type and the smallest for *matPΔC* cells (Figure 5A). However, on average, the delay between the first constriction of the nucleoid and the centralization of the MatP focus was zero in all strains (Figure 5B). Thus, the deletions of *zapA*, *zapB* and *matPΔC* had no significant effect on the onset of constriction of the nucleoid.

The initial constriction at the nucleoid center was frequently transient. The permanent constrictions, which were present uninterrupted until cells divided, appeared in all strains only after the Ter region centralized (Figure 5C). The appearance of the permanent constrictions was significantly delayed in the *ΔzapA* and *ΔzapB* strains compared to the others. The distinction between the *matPΔC*, and the *ΔzapA* and *ΔzapB* strains was also evident in comparing the duration of the localization of the MatP-YPET focus at the center of the nucleoid (Figure 5D). In wild-type cells, the focus stays at the nucleoid center for about 64% of the doubling time. This time drops to 45% for *ΔzapA* and *ΔzapB* cells, and to 28% for *matPΔC* cells. Clearly, a link to the divisome is essential for the extended stay of the Ter region at the center of the nucleoid. Significantly different times for the Ter region to remain centralized in *ΔzapA* and *ΔzapB* strains compared to *matPΔC* strain indicate that in addition to divisome link, MatP mediated inter-chromosomal cross-links may also be important in stabilizing the Ter region at the center of the nucleoid.

Visible constriction of the nucleoid ahead of the Ter centralization is also present in fast growing cells in LB medium (Figure 6). This conclusion is based on static cell images because the high auto-fluorescent background in LB has prevented us from following the MatP-YPET focus through-

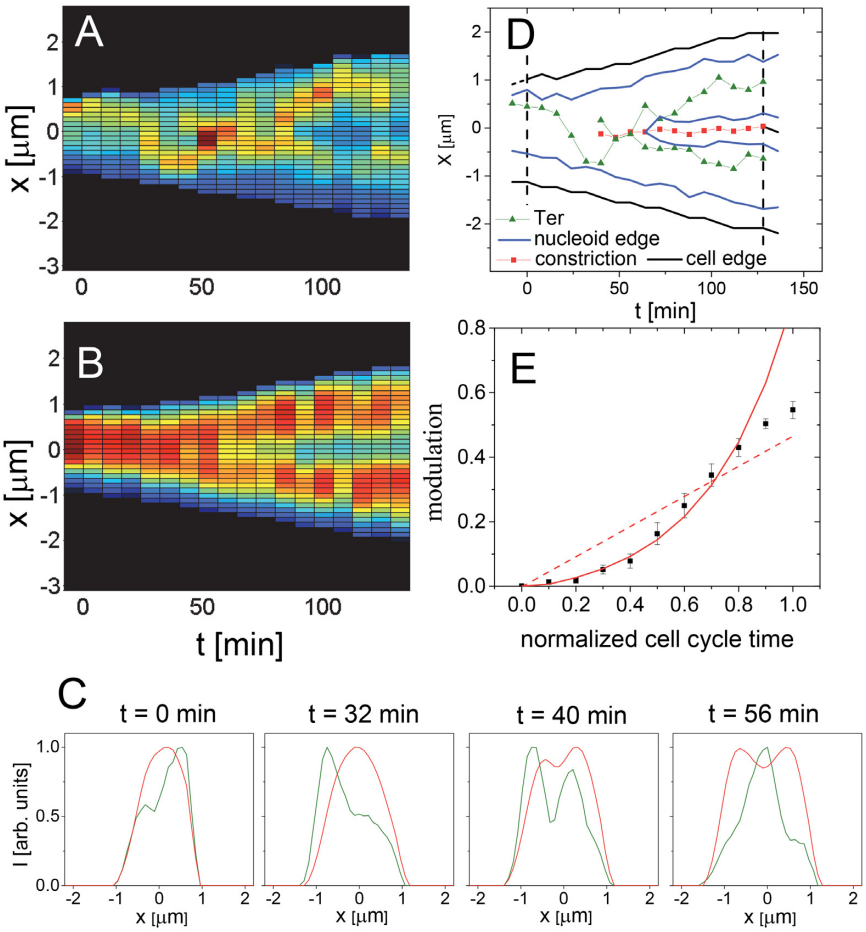

Figure 4. Dynamics of the MatP-YPET focus and chromosome in *matPΔC* cells. (**A** and **B**) Intensity distribution of MatP-YPET and HupA-mCherry, respectively, along long axis for a representative cell during one cell cycle. (**C**) Intensity line profiles and (**D**) contours of cell edges (black solid line), nucleoid edges (blue solid lines), centroids of MatP-YPET labeled Ter regions (filled triangles) and locations of minima in chromosomal densities (red squares) for the same cell. (**E**) Normalized depth of the minimum in intensity distribution of nucleoid label at the center of the nucleoid as a function of normalized cell cycle time. Data are an average from 16 time-lapse sequences from different cells. Error bars represent s.e.m. Solid line is exponential and dashed line linear fit.

out the cell cycle. Unlike slow growing cells in a M9 glycerol medium, the nucleoids in fast growing wild-type cells show a narrow neck-like bridge connecting two chromosome masses before these masses finally separate (Figure 6, center column). The neck-like bridge has also been observed earlier (30,31). Here our two-color imaging shows additionally that the narrow stretched-out chromosomal region co-localizes with the MatP-YPET label, and thus corresponds to the replication terminus region (Figure 6, left column). The neck-like structure was also visible in the *matPΔC* strain (Figure 6B), but we were not been able to observe it in *ΔzapA* and *ΔzapB* cells. The latter two strains are typically more elongated and contain more chromosomal material when growing in a LB medium. The neck-like structure also co-localizes with the MatP-YPET label in the *matPΔC* strain. Importantly, in many instances two additional lobes on both sides of the neck-like structure can be seen (pointed by arrowheads in Figure 6). Unlike in slow growth conditions, these lobes become visible even before the daughter chromosomes separate from each other. Consequently, the bi-lobed nucleoid morphology also precedes the centralization of the Ter region in fast growth conditions in wild-type cells, and this order of events is not specific to slow growth.

Modeling the centralization of the Ter region and chromosomal density distribution

To gain further understanding of the mechanisms that can lead to the centralization of the Ter region and the formation of the mid-nucleoid constriction, we compared the experimental results to a common polymer physics model of DNA (for details see 'Materials and Methods' section). Our approach follows closely that by Jun *et al.* (23,25,32), which has yielded a prediction that two polymer chains in a cylindrical volume can spontaneously segregate due to random thermal motion. Here we follow how a partially replicated chromosome equilibrates in a cylindrical confinement (Figure 7A). At the beginning of each simulation we place the Ter region of such model chromosome at the vicinity of a capped end of a cylinder. We then record the center-of-mass movement of the Ter region (Figure 7B and C, Left), and chromosomal density distribution along the long axis of the cell (Figure 7B and C, Right) as the chain equili-

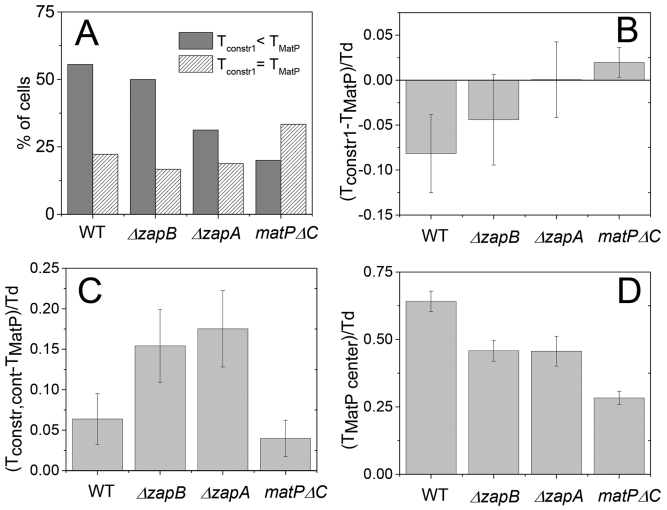

Figure 5. Timing of constriction formation and centralization of the MatP focus. (**A**) Fraction of cells where the first appearance of constriction in the nucleoid center precedes (solid fill), and coincides (hatch) with the centralization of the MatP focus. The respective times are indicated by $T_{constr1}$ and T_{MatP}. (**B**) Time difference between the first appearance of constriction at the nucleoid center and centralization of the MatP focus. (**C**) Time difference between the continuous presence of the constriction at the nucleoid center ($T_{constr,cont}$) and centralization of the MatP focus. (**D**) Times that MatP focus spends at the center of nucleoid ($T_{MatP\ center}$). All times are normalized by doubling times. The average time and s.e.m are shown for each strain. The number of time-lapse sequences analyzed are 18, 18, 16 and 15 for WT, Δ*zapB*, Δ*zapA* and *matPΔC* strains, respectively.

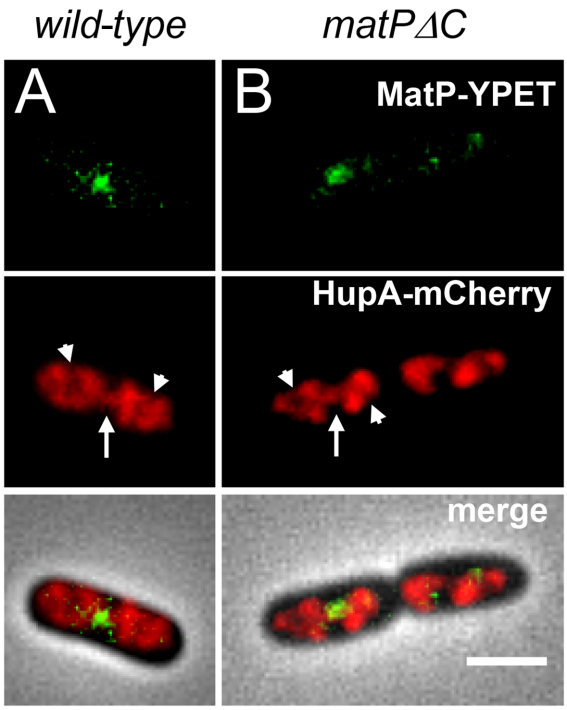

Figure 6. MatP focus and chromosomes in fast growth conditions. Examples of (**A**) wild-type and (**B**) *matPΔC* cells in a LB medium that show characteristic bridges between two chromosomal masses (pointed to by upward arrows). Arrowheads point to constrictions in a nucleoid distribution away from the MatP-YPET focus. In the merged image, two fluorescent images have been overlaid by phase contrast image. Scale bar is 2 μm.

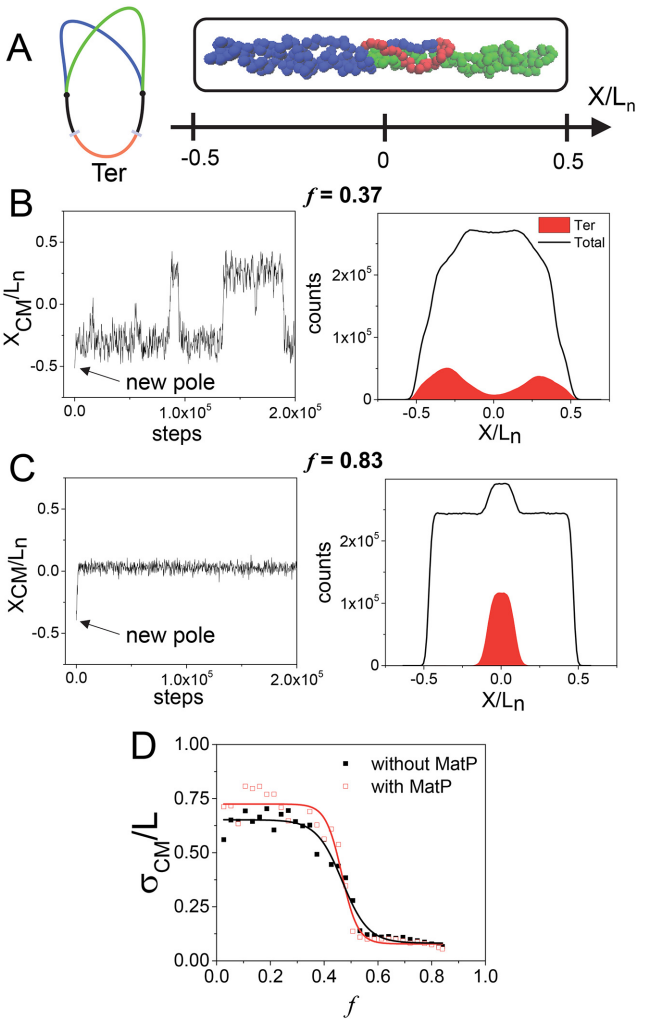

Figure 7. Coarse-grained molecular dynamics modeling of the replication terminus region and the whole chromosome. (**A**) Left: a partially replicated chromosome is modeled that consists of two replicated chains connected by unreplicated chain. Right: a snapshot of the model chromosome that has been equilibrated in a cylindrical confinement. This chromosome has all but the Ter region replicated ($f = 0.83$). Ter region is colored red and replicated chromosome arms blue and green. (**B**) Left: center-of-mass movement of the replication terminus region, which starts from the new pole. The horizontal axis is in molecular dynamics steps. The vertical axis is normalized by the length of the nucleoid (L_n). Right: time averaged distributions of the replication terminus region (red filled curve) and the whole chromosome (black solid line). Replicated fraction $f = 0.37$. (**C**) Same for replicated fraction $f = 0.83$. (**D**) Standard deviation of center-of-mass position as a function of replicated fraction. Small standard deviation corresponds to centralized Ter region. Solid (open) symbols correspond to the model without (with) cross-linking effects. The lines represent sigmoidal fits with their midpoint at $f = 0.47$.

brates. Both center of mass and density distributions can be directly compared to experimental results presented in Figures 3 and 4. However, the modeling time step here is not linked to the actual measurement time and therefore the model is only able to predict qualitatively the kinetics of the chain.

First, we investigate the centralization of the Ter region in the model chromosome without MatP related cross-linking effects. We carry out equilibration of the chain for different

fractions of replicated DNA (f). Here, the replicated fraction f is defined to vary between zero and one; $f = 1$ corresponds to two fully replicated chromosomes, and $f = 0$ to a single not yet replicated one. When the replicated fraction of the chromosome is small, the Ter region remains preferentially localized at a cell pole but it can also move rapidly between the poles (Figure 7B, Left). These movements show similarity to the experimental data from the *matP*ΔC strain, where Ter movement between poles was observed in the early part of the cell cycle (cf. Figure 4). Further progression of replication leads to localization of the Ter region at the center of the nucleoid (Figure 7C). In this configuration the two replicated chromosome chains are separated from each other by the Ter region, which situates between them at the center of the cell (cf. Figure 7A, Right). The transition to this configuration occurs when approximately half of the chromosome is replicated (Figure 7D). The model predicts that the Ter region stays then centralized until it is fully replicated.

While successfully explaining the experimentally observed centralization of the Ter region, the model completely fails to predict a constriction at the center of the nucleoid prior to or concurrently with the centralization. Instead of a minimum, the model produces a maximum in the chromosome density distribution at the nucleoid center (Figure 7C, Right). The maximum arises because of DNA topology. In the maximum region at least three DNA chains, two replicated and the yet to be replicated one, must overlap (cf. Figure 7A, Right). Further from the Ter region, only two newly replicated chains need to be present and therefore the overall nucleoid density is lower there. The maximum remains also present when the polymer chain is not confined by the end gaps of the cylinder, i.e. in a very long cylinder. A local maximum at the center of the nucleoid persisted also when we introduced a constant external force to the model that pushed two newly formed chromosomal masses apart from each other toward the cell poles (Supplementary Figure S7A). Although in the current model the force is of hypothetical origin, it has been reported that the Min system exerts such an effective force on the chromosome (33). We found that the local maximum only disappeared and gave rise to local minimum after the Ter region was completely replicated, i.e. when two unlinked ring polymers were present in the cell. In this case the local minimum was present even without the force (Supplementary Figure S7B and C).

Lastly, we investigate the effect of MatP cross-linking to Ter centralization and on chromosomal density distribution in the model chromosome. To account for cross-linking, we use an effective attractive potential between the monomers in the Ter region. A similar approach has been adopted recently by Junier *et al.* (34). We choose the strength of the potential so that it compacts the Ter region in the longitudinal direction to 2/3 of its original size (Supplementary Figure S8) matching approximately our experimental observations (Figure 2B). Simulations with a compacted Ter region show that compaction has only a minimal effect on Ter centralization, which still occurs when approximately half of the chromosome has been replicated (Figure 7D). Moreover, we found that the cross-linking did not significantly affect chromosomal density distribution along the long axis of the cell for replication fractions $f > 0.5$. As in the un-crosslinked case, the model fails to account for the minimum in the density distribution at the center of the nucleoid, and instead it predicts a maximum (Supplementary Figure S9).

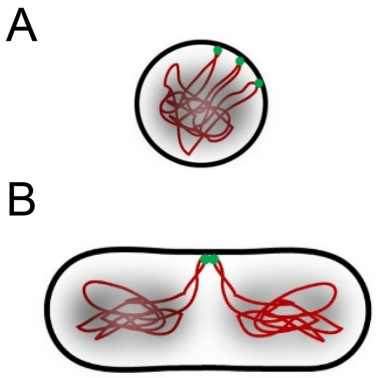

Figure 8. Schematic organization of the Ter region in WT cells. (**A**) Cross-sectional view of chromosomes perpendicular to the long axis of the cell at the location of the divisome. The Ter region is attached to the divisome via the Ter linkage (green dots) along a segment at the cell perimeter. (**B**) Cross-sectional view of the chromosomes along the long axis of cell. Chromosomes are attached to the divisome at *matS* sites and only sequences in the vicinity of *matS* are localized at the center of the cell.

DISCUSSION

Organization of the Ter region

Several reports indicate that the Ter region is linked to the divisome via MatP, ZapA and ZapB (18,20). Our analysis has provided further support for the existence of this link showing that MatP fluorescently labeled foci are on average elongated along the short axis of the cell, which is consistent with the idea that this chromosomal region is attached to the divisome. Although previous reports have not reported lateral elongation (15,18,20) here we observe it using two different labeling schemes based on YPET and mCherry fusions to MatP C-terminus. It is possible that the spread of the MatP focus along the short axis of cell depends on the functionality of the MatP-fluorescent protein construct. A more functional fusion construct is likely to have a stronger attachment to the divisome over a more extended region resulting in an elongated appearance of the foci in microscopic images. However, our data show also only limited attachment of the Ter region which does not span the whole divisome. We think that this finding is not a consequence of the limited functionality of the fusion construct, but is related to the organization of the Ter region itself. If the Ter region were to contact the divisome in multiple separate points, we should have observed individual foci along the short axes of cell but this was not the case. Thus, our data show that the linking does not occur uniformly throughout the perimeter of the cell, but only within a sub-region of it (Figure 8A).

There has been an ongoing discussion about how the Ter region is spread along the long axis of the cell in *E. coli*. By one view, the Ter region is spread out throughout the nucleoid (9–11). By an opposing view, it is more compacted

than the rest of the chromosome (13–15). Our data provide clues as to how to reconcile these two contradictory views. We observe that bulk nucleoid masses separate from each other exponentially in time. This exponential separation also applies to the center region of the nucleoid. The latter finding contradicts the idea that the whole Ter region remains fixed at the center of the cell after its replication. The Ter region comprises a sizeable portion of the whole chromosome (about 18%). Such a large amount of the chromosomal mass is not present at mid-cell during the late stages of the cell cycle, even though the MatP-YPET label still resides there. We propose that the majority of DNA in the Ter region also moves away from the center of the cell, and only leaves behind stretched-out segments with *matS* sites, which attach to the divisome via Ter linkages (Figure 8B).

Differential effect of MatP compared to ZapA and ZapB in organizing the Ter region

For the Ter linkage to form ZapA, ZapB and MatP all need to be present. However, deletion of *zapA* or *zapB* has a smaller effect on the longitudinal spread of the Ter region compared to the deletion of *matPΔC* (Figure 2B). We interpret the difference between MatP, and ZapA and ZapB as arising from the capability of MatP to cross-link DNA within the nucleoid through *matS* sites in addition to its role in linking the Ter region to the divisome, while ZapA and ZapB only participate in the latter link. Additionally, MatP can possibly cross-link DNA belonging to two different daughter chromosomes, which may also effectively reduce the longitudinal spread of the Ter region. Further evidence for intra-chromosomal MatP cross-links is provided by the finding that in *matPΔC* the replication terminus region spends less time at the center of the nucleoid than in Δ*zapA* and Δ*zapB* strains (Figure 5C).

Differential effect of MatP compared to ZapA and ZapB in bulk chromosome segregation

The appearance of a bi-lobed nucleoid morphology is indicative of ongoing chromosome partitioning into new daughter cells (30,31,35). Our study reveals that the bi-lobed nucleoid morphology, i.e. continuously observable constriction, appears at the center of the nucleoid in all imaged strains after centralization of the Ter region (Figure 5C). Interestingly, deletion of *zapA* or *zapB* leads to a delay in the permanent constriction formation, while a C-terminal deletion of *matP* has no such effect. Also, in the former two strains, narrow neck-like bridges between two chromosomal masses are not observable in fast growth conditions, while this distinct structural motif appears clearly in the *matPΔC* strain. Thus, there is a defect in bulk chromosome segregation in *ΔzapA* and *ΔzapB* strains, but not in a *matPΔC* strain. It is possible that in *ΔzapA* and *ΔzapB* strains, MatP-MatP cross-links are holding chromosomes together, and this cross-linking hinders bulk chromosome segregation. These cross-links are absent in a *matPΔC* strain, and they are possibly less frequent in wild-type cells, because some MatP-decorated *matS* sites are involved in linking these sites to the divisome. Clearly, ZapB and ZapA can influence chromosomal segregation and organization also by other direct or indirect mechanisms. For example, these abundant proteins could contribute to osmotic compaction of the chromosome.

Entropic force can drive centralization of the Ter region in high volume fractions of DNA

The replication terminus region has been known to move independently of the divisome from the periphery to the center of the nucleoid before being replicated (17,18). Jun *et al.* have proposed that when the chromosome is more than half way replicated, the unreplicated part of the chromosome positions itself spontaneously at the center of the nucleoid (23). Our modeling has confirmed this finding and furthermore predicted that compaction of the replication terminus region by MatP, or some other cross-linking agents, has a minimal effect on the centralization. The latter result is in accord with our experimental findings.

It is important to note that the model predicts centralization of the Ter region only when the chromosomal volume fraction within the nucleoid volume is high. At lower volume fractions, the entropic force alone is not sufficient to position the Ter region (34). The effective volume fraction, which enters coarse grain models, depends on a variety of factors such as supercoiling, which increases the effective volume fractions and topoisomerase strand exchange activity, which effectively decreases it by allowing the strands to pass through each other (36). The relative strength of these effects is yet to be quantified. Given that the experiment and the model agree, it is possible that the assumption entering the model, namely that DNA within the nucleoid is compacted to a high effective volume fraction, holds.

Mid-nucleoid constriction of chromosomes proceeds despite entropic force and the Ter linkages

Although the computational model captures the centralization of the Ter region, it fails to reproduce chromosomal density distribution at the center of the nucleoid at the time of this transition. The inability of the model to reproduce this key aspect of the experimental data indicates that instead of conformational entropy, some other process drives constriction formation and separation of two daughter nucleoids. What can be the underlying process? Several systems have been implicated in moving and segregating DNA in *E. coli* in the past. For example, DNA translocase FtsK can clear chromosomal masses from the septum region (37). However, FtsK mediated translocation appears only at the late stage of the cell cycle when the division septum is about to close (38). Considering very different timing, FtsK related DNA pumping is unlikely to explain the formation of a constriction at the center of the nucleoid ahead of the centralization MatP focus. Several reports have implied that the Min system plays role in chromosome segregation (33,39,40) in addition to its well-known function of localizing the cell division plane. Recently, Ventura *et al.* combined modeling and experiment, and showed that MinD in *E. coli* can tether DNA to the membrane in an ATP-dependent manner, and these dynamic links can lead to chromosome segregation and separation due to the non-uniform distri-

bution of Min proteins on the cell membrane (33). These authors performed their measurements in fast growth conditions. In slow growth conditions, however, only a minor defect in chromosome segregation appears and constrictions in the nucleoids can still be observed (17). Thus, the Min system facilitates the segregation process but its presence is not necessary for the formation of the constriction at the center of the nucleoid, and the separation of the two daughter chromosomes.

The observation that nucleoid edges maintain approximately constant distances from the cell poles, and that the nucleoid length increases exponentially in time as the cell grows, indicate that chromosomal segregation is linked to cell growth. Transertion, i.e. coupled transcription, translation and transertion (41–43), has been proposed as a possible mechanism that links cell growth and nucleoid expansion. Severing transertional linkages by short treatment by chloramphenicol, or by rifampicin, leads to compaction of nucleoids (44), in accord with this idea. However, it was found that transcriptional inactivation by rifampicin did not prevent the segregation of chromosomal loci (12,45). Moreover, the separation of origins occurs at a much faster rate than cell growth (45). Accordingly, a transertional mechanism cannot be responsible for early stages of chromosomal segregation, but its involvement in later stages of the segregation process remains a possibility that deserves further attention.

In summary, our study has shown that bulk chromosome segregation leads to the formation of two distinct chromosomal masses before centralization of the replication terminus region. This process occurs largely independently of the MatP C-terminal domain, and ZapA and ZapB. Once the Ter region has centralized and the divisome has formed, a link between the two is established via ZapA, ZapB and MatP proteins. Thanks to this link, *matS* sites in the Ter region remain fixed at mid-cell even though the two bulk chromosomal masses move apart at comparable speed to cell elongation. The exact nature of the process that drives the two newly formed chromosomal masses apart remains an important open question for future studies.

SUPPLEMENTARY DATA

Supplementary Data are available at NAR Online.

ACKNOWLEDGEMENTS

The authors thank Ryan A. Hefti, Cynthia U. Nkem and Alex M. Hill for the help at the initial stages of the project, John Marko, Conrad Woldringh and Arieh Zaritsky for useful discussions, and Anna Jennings and Matthew W. Bailey for the critical reading of the manuscript. The authors acknowledge technical assistance and material support from the Center for Environmental Biotechnology at the University of Tennessee.

FUNDING

University of Tennessee start-up funds (in part); National Science Foundation [MCB-1252890]. Part of this research was conducted at the Center for Nanophase Materials Sciences, which is sponsored at Oak Ridge National Laboratory by the Scientific User Facilities Division, Office of Basic Energy Sciences, U.S. Department of Energy. Funding for open access charge: University of Tennessee start-up funds.

Conflict of interest statement. None declared.

REFERENCES

1. Wang,X., Llopis,P.M. and Rudner,D.Z. (2013) Organization and segregation of bacterial chromosomes. *Nat. Rev. Genet.*, **14**, 191–203.
2. Postow,L., Hardy,C.D., Arsuaga,J. and Cozzarelli,N.R. (2004) Topological domain structure of the *Escherichia coli* chromosome. *Genes Dev.*, **18**, 1766–1779.
3. de Vries,R. (2010) DNA condensation in bacteria: Interplay between macromolecular crowding and nucleoid proteins. *Biochimie*, **92**, 1715–1721.
4. Odijk,T. (1998) Osmotic compaction of supercoiled DNA into a bacterial nucleoid. *Biophys. Chem.*, **73**, 23–29.
5. Pelletier,J., Halvorsen,K., Ha,B.-Y., Paparcone,R., Sandler,S.J., Woldringh,C.L., Wong,W.P. and Jun,S. (2012) Physical manipulation of the *Escherichia coli* chromosome reveals its soft nature. *Proc. Natl. Acad. Sci. U.S.A.*, **109**, E2649–E2656.
6. Dillon,S.C. and Dorman,C.J. (2010) Bacterial nucleoid-associated proteins, nucleoid structure and gene expression. *Nat. Rev. Microbiol.*, **8**, 185–195.
7. Wang,W.Q., Li,G.W., Chen,C.Y., Xie,X.S. and Zhuang,X.W. (2011) Chromosome organization by a nucleoid-associated protein in live bacteria. *Science*, **333**, 1445–1449.
8. Toro,E. and Shapiro,L. (2010) Bacterial chromosome organization and segregation. *Cold Spring Harb. Perspect. Biol.*, **2**, a000349.
9. Reyes-Lamothe,R., Wang,X. and Sherratt,D.J. (2008) *Escherichia coli* and its chromosome. *Trends Microbiol.*, **16**, 238–245.
10. Wiggins,P.A., Cheveralls,K.C., Martin,J.S., Lintner,R. and Kondev,J. (2010) Strong intranucleoid interactions organize the *Escherichia coli* chromosome into a nucleoid filament. *Proc. Natl. Acad. Sci. U.S.A.*, **107**, 4991–4995.
11. Wang,X.D., Liu,X., Possoz,C. and Sherratt,D.J. (2006) The two *Escherichia coli* chromosome arms locate to separate cell halves. *Genes Dev.*, **20**, 1727–1731.
12. Woldringh,C.L., Hansen,F.G., Vischer,N.O.E. and Atlung,T. (2015) Segregation of chromosome arms in growing and non-growing *Escherichia coli* cells. *Front. Microbiol.*, **6**, 448.
13. Niki,H., Yamaichi,Y. and Hiraga,S. (2000) Dynamic organization of chromosomal DNA in *Escherichia coli*. *Genes Dev.*, **14**, 212–223.
14. Valens,M., Penaud,S., Rossignol,M., Cornet,F. and Boccard,F. (2004) Macrodomain organization of the *Escherichia coli* chromosome. *EMBO J.*, **23**, 4330–4341.
15. Mercier,R., Petit,M.-A., Schbath,S., Robin,S., El Karoui,M., Boccard,F. and Espeli,O. (2008) The MatP/matS site-specific system organizes the terminus region of the *E. coli* chromosome into a macrodomain. *Cell*, **135**, 475–485.
16. Dupaigne,P., Tonthat,N.K., Espeli,O., Whitfill,T., Boccard,F. and Schumacher,M.A. (2012) Molecular basis for a protein-mediated DNA-bridging mechanism that functions in condensation of the *E. coil* chromosome. *Mol. Cell*, **48**, 560–571.
17. Bailey,M.W., Bissichia,P., Warren,B.T., Sherratt,D.J. and Männik,J. (2014) Evidence for divisome localization mechanisms independent of the Min system and SlmA in *Escherichia coli*. *PLoS Genet.*, **10**, e1004504.
18. Espeli,O., Borne,R., Dupaigne,P., Thiel,A., Gigant,E., Mercier,R. and Boccard,F. (2012) A MatP-divisome interaction coordinates chromosome segregation with cell division in *E. coli*. *EMBO J.*, **31**, 3198–3211.
19. Männik,J. and Bailey,M.W. (2015) Spatial coordination between chromosomes and cell division proteins in *Escherichia coli*. *Front. Microbiol.*, **6**, 306.
20. Buss,J., Coltharp,C., Shtengel,G., Yang,X., Hess,H. and Xiao,J. (2015) A multi-layered protein network stabilizes the *Escherichia coli* FtsZ-ring and modulates constriction dynamics. *PLoS Genet.*, **11**, e1005128.

21. Galli,E. and Gerdes,K. (2010) Spatial resolution of two bacterial cell division proteins: ZapA recruits ZapB to the inner face of the Z-ring. *Mol. Microbiol.*, **76**, 1514–1526.
22. Galli,E. and Gerdes,K. (2012) FtsZ-ZapA-ZapB Interactome of *Escherichia coli*. *J. Bacteriol.*, **194**, 292–302.
23. Jun,S. and Mulder,B. (2006) Entropy-driven spatial organization of highly confined polymers: lessons for the bacterial chromosome. *Proc. Natl. Acad. Sci. U.S.A.*, **103**, 12388–12393.
24. Guberman,J.M., Fay,A., Dworkin,J., Wingreen,N.S. and Gitai,Z. (2008) PSICIC: Noise and asymmetry in bacterial division revealed by computational image analysis at sub-pixel resolution. *PLoS Comput. Biol.*, **4**, e1000233.
25. Arnold,A. and Jun,S. (2007) Time scale of entropic segregation of flexible polymers in confinement: Implications for chromosome segregation in filamentous bacteria. *Phys. Rev. E*, **76**, 031901.
26. Jun,S. and Wright,A. (2010) Entropy as the driver of chromosome segregation. *Nat. Rev. Microbiol.*, **8**, 600–607.
27. Romantsov,T., Fishov,I. and Krichevsky,O. (2007) Internal structure and dynamics of isolated *Escherichia coli* nucleoids assessed by fluorescence correlation spectroscopy. *Biophys. J.*, **92**, 2875–2884.
28. Limbach,H.J., Arnold,A., Mann,B.A. and Holm,C. (2006) ESPResSo—an extensible simulation package for research on soft matter systems. *Comput. Phys. Commun.*, **174**, 704–727.
29. Fisher,J.K., Bourniquel,A., Witz,G., Weiner,B., Prentiss,M. and Kleckner,N. (2013) Four-dimensional imaging of *E. coli* nucleoid organization and dynamics in living cells. *Cell*, **153**, 882–895.
30. Yazdi,N.H., Guet,C.C., Johnson,R.C. and Marko,J.F. (2012) Variation of the folding and dynamics of the *Escherichia coli* chromosome with growth conditions. *Mol. Microbiol.*, **86**, 1318–1333.
31. Bates,D. and Kleckner,N. (2005) Chromosome and replisome dynamics in *E. coli*: loss of sister cohesion triggers global chromosome movement and mediates chromosome segregation. *Cell*, **121**, 899–911.
32. Jung,Y., Jeon,C., Kim,J., Jeong,H., Jun,S. and Ha,B.-Y. (2012) Ring polymers as model bacterial chromosomes: confinement, chain topology, single chain statistics, and how they interact. *Soft Matter*, **8**, 2095–2102.
33. Di Ventura,B., Knecht,B., Andreas,H., Godinez,W.J., Fritsche,M., Rohr,K., Nickel,W., Heermann,D.W. and Sourjik,V. (2013) Chromosome segregation by the *Escherichia coli* Min system. *Mol. Syst. Biol.*, **9**, 686.
34. Junier,I., Boccard,F. and Espeli,O. (2014) Polymer modeling of the *E. coli* genome reveals the involvement of locus positioning and macrodomain structuring for the control of chromosome conformation and segregation. *Nucleic Acids Res.*, **42**, 1461–1473.
35. Joshi,M.C., Bourniquel,A., Fisher,J., Ho,B.T., Magnan,D., Kleckner,N. and Bates,D. (2011) *Escherichia coli* sister chromosome separation includes an abrupt global transition with concomitant release of late-splitting intersister snaps. *Proc. Natl. Acad. Sci. U.S.A.*, **108**, 2765–2770.
36. Lampo,T.J., Kuwada,N.J., Wiggins,P.A. and Spakowitz,A.J. (2015) Physical modeling of chromosome segregation in escherichia coli reveals impact of force and DNA relaxation. *Biophys. J.*, **108**, 146–153.
37. Stouf,M., Meile,J.-C. and Cornet,F. (2013) FtsK actively segregates sister chromosomes in *Escherichia coli*. *Proc. Natl. Acad. Sci. U.S.A.*, **110**, 11157–11162.
38. Kennedy,S.P., Chevalier,F. and Barre,F.-X. (2008) Delayed activation of Xer recombination at dif by FtsK during septum assembly in *Escherichia coli*. *Mol. Microbiol.*, **68**, 1018–1028.
39. Akerlund,T., Gullbrand,B. and Nordstrom,K. (2002) Effects of the Min system on nucleoid segregation in *Escherichia coli*. *Microbiology*, **148**, 3213–3222.
40. Jia,S., Keilberg,D., Hot,E., Thanbichler,M., Sogaard-Andersen,L. and Lenz,P. (2014) Effect of the Min system on timing of cell division in *Escherichia coli*. *PLoS One*, **9**, e103863.
41. Norris,V. (1995) Hypothesis—chromosome separation in *Escherichia coli* involves autocatalytic gene expression, transertion and membrane-domain formation. *Mol. Microbiol.*, **16**, 1051–1057.
42. Matsumoto,K., Hara,H., Fishov,I., Mileykovskaya,E. and Norris,V. (2015) The Membrane: transertion as an organizing principle in membrane heterogeneity. *Front. Microbiol.*, **6**, 572.
43. Woldringh,C.L. (2002) The role of co-transcriptional translation and protein translocation (transertion) in bacterial chromosome segregation. *Mol. Microbiol.*, **45**, 17–29.
44. Bakshi,S., Choi,H., Mondal,J. and Weisshaar,J.C. (2014) Time-dependent effects of transcription- and translation-halting drugs on the spatial distributions of the *Escherichia coli* chromosome and ribosomes. *Mol. Microbiol.*, **94**, 871–887.
45. Wang,X. and Sherratt,D.J. (2010) Independent segregation of the two arms of the *Escherichia coliori* region requires neither RNA synthesis nor MreB dynamics. *J. Bacteriol.*, **192**, 6143–6153.